

NUMERICAL STUDY OF HEAT TRANSFER ENHANCEMENT BY INSERTING DIFFERENT SIZE BALLS INSIDE TUBE

*Haider L. Aneed¹Dhamyaa S. Khudhur¹

1) Mechanical Engineering Department, College of Engineering, Mustansiriyah University, Baghdad, Iraq

Received 30/3/2021

Accepted in revised form 29/5/2021

Published 1/11/2021

Abstract: In this paper, the challenge is to increasing of the heat exchanger performance by placing different size balls inside the tubes. the development of previous studies to enhance relatively bad case of heat transfer where the inserting (a large ball and then a small ball) to collide the water molecules in the ball and generate turbulent flow (Reynolds number range from 50,000 to 350,000) and thus increase the thermal performance due to collision of particles with the inner casing of the tube and reduce the stagnation near the wall. The usefulness of small ball, after the big ball, is Reduce of gets wake flow. A simulation was made when changing the diameter ratio of big to small ball ($Dr = 3, 4, 5$). Also, the distance between the big ball and the small ball was changed ($X = 2, 3, 5$) mm. It was concluded that the best ball diameter ratio and best Distance is ($Dr = \frac{D_b}{D_{sb}} = 5$), ($X = 3$ mm), respectively. The pressure drop acts as a side effect of enhancement. Therefore, the method of equal pumping was adopted. The average thermal performance factor (TPF=1.178) of tube with insert the balls enhanced by 17.8% at ($x=3$ mm) and ($Dr=5$) when compared with smooth tube.

Keywords: diameter ratio, thermal performance factor, ball insert

1. Introduction

Improving heat transfer in heat exchangers is the goal of designers and researchers by using different methods and designs. There are several ways to improve thermal performance in heat exchangers and classify these methods according to their energy exchange, namely: passive

methods, active methods, and combined methods) [1]. In passive methods, no need to external power, while in active methods an outer energy source is required to complete the performance improvement process, and the combined method is a mix between the previous two methods and its purpose is to reach the highest performance of the heat exchanger [2].

There are a lot of researchers used the passive technology by inserting different objects into the tubes. The most widely used method is by sticking a twisted strip into the tube because of its ease of manufacture and high performance [3]. The principle of working the passive method is that when the stagnation increases near the wall of the tube, this layer of fluid acts as insulation and the amount of heat transferred will reduce. The insertion of geometry acts as vortex generator to collapse of the stagnation state within the fluid layers near the wall, but at the same time there will be an increase in the pressure drop that needs additional energy to overcome this pressure drop increase [4].

The effect of adding geometric objects can be negative for thermal performance that is when

*Corresponding Author: haider.lafta@duc.edu.iq

inserting the object; the case needs a pumping power to overcome the large pressure drop that occurred as a result of the insertion is higher than the increase in the amount of heat transferred through the tube. Therefore, there must be a term that is specified the case whether it is an increase or a decrease in thermal performance, this term is called as *thermal performance factor (TPF)* [5]

The best way to find the value of the thermal performance factor is a method of equal pumping power in which the increase in the amount of heat transferred as a result of adding an object inside the tube is compared with the amount of increase in pressure drop as a result of that body being trapped in the tube.

The purpose of this research paper is to improve the thermal performance of water-cooled heat exchangers. In this study, a numerical simulation of a circular stream containing fixed balls of different sizes for the Reynolds number range from 50,000 to 350,000. Dimensions ratios were chosen in order for the study to apply to all industrial units.

F. Andrade. et. al. [6] conducted an experimental study by developing corrugated tubes and comparing them with smooth tube, the same dimension was chosen for each tube of 5.75 mm in diameter and length of 0.38 m. The practical tests were applied in three regimes (laminar, transitional and turbulent). The data showed in the corrugated tube, the friction factor at transition regime is less as compared with smooth tube. The maximum increase in heat transfer at $Re = 2000$, specifically, the Nusselt number ratio $\{Nu/Nu_s\}$ increases up to 4.7

Pengxiao Li, et. al. [7] studied practically and numerically the heat transfer and flow performance in turbulent flow with the drainage inserts inside tube. The results showed a good blending of fluid layers. The experiment analysis examination the effect of pitch to diameter ratio

on the Nusselt number and friction factor, The Nusselt number and friction factor boost with the decrease of pitch to diameter ratio. The results show that the best angle of slant is 45° for the inserting of the geometry which is shown in figure (1).

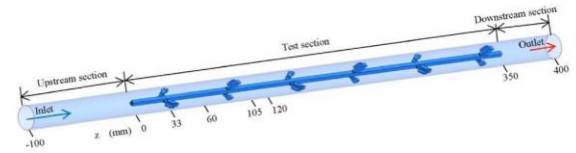


Figure 1. Schematic diagram of the computation domain

Changzhong Man, et. Al [8] studied the heat transfer and friction characteristics of dual - pipe heat exchanger. The insert geometry is twisted tape with alternation of clockwise and counterclockwise twisted tape (ACCT tape) and typical twisted tape (TT tape), as shown in the figure (2).

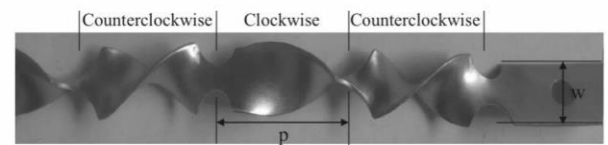


Figure 3. Clockwise and counterclockwise twisted tape

The results reveal the ACCT tapes have better thermal performance than the typical twisted tapes, the maximum value of thermal performance factor is 1.42 at full - length (1 - 2400 mm) ACCT.

Shyy Woei Chang, et. al. [9] conducted an enhanced Heat Transfer by made a grooved or/and ribbed square wire coils insert inside tube. The investigation experimentally examined. Five pitch ratios of wire coils (P/d) of 0.5, 1, 1.5, 2 and 2.5 are tested at Reynolds numbers (Re) range from 10,000 to 40,000. The unstable separation was dispersed in the flow by ribs; the jet of the flow destroyed by the trigger of grooves the complex and cyclic eddy association with the

axial swirl to increase thermal performance from the smooth-coil tube. The thermal performance factor values of this study conditions are all above than one.

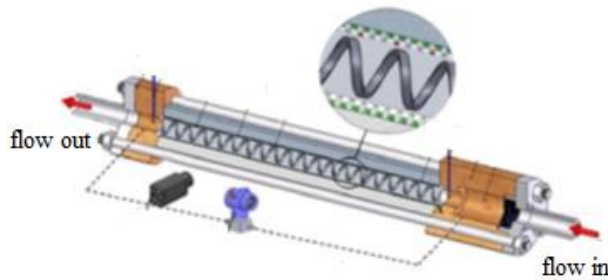


Figure 4. Grooved and ribbed square wire coils insert inside tube

In the concept of previous studies as mentioned in Table (1), where all studies indicate the existence of a group of factors and influences that are responsible for the process of improving thermal performance, as there is still an improvement in heat transfer with the least resistance to flow, therefore, a new arrangement are developing for large and small balls to give a better heat transfer performance.

2. Geometry and case study

In this paper, different sized balls were used inside the tube, as shown in the figure (5), where a small ball is behind every large ball. Two parameters were changed at range of Reynolds number (50,000 to 350,000). First parameter is the diameter ratio between large ball and small ball ($D_r = D_b/D_{sb} = 3, 4, \text{ and } 5$) and the second changed parameter is the distance between large ball and small ball ($x = 2, 3, \text{ and } 5 \text{ mm}$). The rest of the parameters remain constant like distance between two large balls (L) and tube diameter (D_t) and heat flux on the tube.

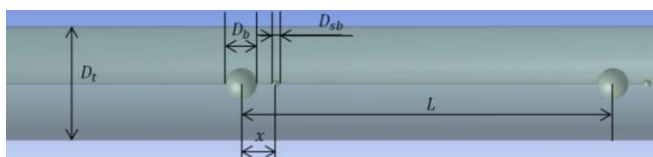


Figure 5. Geometry of the case study

3. Governing Equations

The following equations were used to calculate the number of Nusselt, the equation (1) through the numerical calculation of a certain number of points on the tube, and after that the mean value was extracted for the number of Nusselt in the case of balls inside the tube. Equation (2) is an empirical equation of Nusselt number applied on a smooth tube without an insert of balls from Dittus-Boelter equation [10-11]:

$$Nu = \frac{h \cdot D_t}{\lambda} \quad (1)$$

$$Nu)_s = 0.023 (Re)^{0.8} \cdot (Pr)^{0.4} \quad (2)$$

Where Reynolds number (Re) is proportional to the average velocity (u) and the diameter of the tube D_t :

$$Re = \frac{\rho \cdot u \cdot D_t}{\mu} \quad (3)$$

Numerical calculation of the friction factor was calculated when the balls inside tube from Darcy-Weisbach equation:

$$f = \frac{2 \cdot \Delta p \cdot D_t}{L \cdot \rho \cdot u^2} \quad (4)$$

$$f_s = 0.3164 (Re)^{-0.25} \quad (5)$$

The equation (5) is empirical formula for smooth tube found by Blasius solution.

$$\eta = \frac{Nu/Nu)_s}{(f/f_s)^{1/3}} \quad (6)$$

The equation (6) is thermal performance factor which represented a comparison between tube with insertion of balls and smooth tube; it is based on equal surface area of the heat transfer at equal pumping power.

4. Numerical Method and Boundary Conditions

Simulation is done by software (Fluent 19R1) of the CFD process in which the solution is dependent on finite volume method. Where the simulation of this research is by applying a constant heat flux on the wall of the tube as

shown in the figure (6). And one of the followed hypotheses is that the velocity of the flow is equal to zero at the walls and also fully developed flow with a temperature of the inlet water is constant. The range used for Reynolds number is from 50,000 to 350,000. The criteria of convergence is Prepared on (10^{-6}) for all variables. It is also hypotheses that the thickness of the tube has been neglected, and this means that equation (1) can be used to extract the local Nusselt number for each point of the tube for a given and fixed length, after which the average is calculated for the Nusselt number of the entire tube.

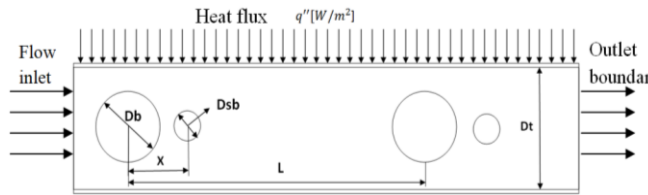


Figure 6. Schematic diagram of boundary conditions

The mathematical model builds up according to applying the boundary conditions on the case study, therefore, the basic equations for fluid flow and the laws of conservation of energy, mass and momentum [12]:

- **Mass conservation**

$$\frac{\partial}{\partial z}(\bar{u}) + \frac{1}{r} \frac{\partial}{\partial r}(r\bar{v}) + \frac{1}{r} \frac{\partial}{\partial \theta}(\bar{w}) = 0 \quad (7)$$

Where: \bar{u} , \bar{v} , \bar{w} represented average velocity components in the directions r , θ , z .

- **Momentum conservation**

In Z direction

$$\rho \left(\frac{\partial U}{\partial t} + U \frac{\partial U}{\partial z} + V \frac{\partial U}{\partial r} + \frac{W}{r} \frac{\partial U}{\partial \theta} \right) = - \frac{\partial p}{\partial z} + \left(\frac{1}{r} \frac{\partial}{\partial r}(r\tau_{rz}) + \frac{1}{r} \frac{\partial}{\partial \theta} \tau_{\theta z} + \frac{\partial}{\partial z} \tau_{zz} \right) + \rho F_z \quad (8)$$

In r direction

$$\rho \left(\frac{\partial V}{\partial t} + U \frac{\partial V}{\partial z} + V \frac{\partial V}{\partial r} + \frac{W}{r} \frac{\partial V}{\partial \theta} - \frac{W^2}{r} \right) = - \frac{\partial p}{\partial r} + \left(\frac{1}{r} \frac{\partial}{\partial r}(r\tau_{rr}) + \frac{1}{r} \frac{\partial}{\partial \theta} \tau_{\theta r} + \frac{\partial}{\partial z} \tau_{zr} - \frac{\tau_{\theta\theta}}{r} \right) + \rho F_r \quad (9)$$

In θ direction

$$\rho \left(\frac{\partial W}{\partial t} + V \frac{\partial W}{\partial r} + \frac{W}{r} \frac{\partial W}{\partial \theta} + \frac{WV}{r} + U \frac{\partial W}{\partial z} \right) = - \frac{1}{r} \frac{\partial p}{\partial \theta} + \left(\frac{1}{r^2} \frac{\partial}{\partial r}(r^2 \tau_{r\theta}) + \frac{1}{r} \frac{\partial}{\partial \theta} \tau_{\theta\theta} + \frac{\partial}{\partial z} \tau_{z\theta} + \frac{\tau_{\theta r} - \tau_{r\theta}}{r} \right) + \rho F_\theta \quad (10)$$

Where:

$$\tau_{rr} = \mu \left(2 \frac{\partial V}{\partial r} - \frac{2}{3} (\nabla \cdot \vec{v}) \right) \quad (11)$$

$$\tau_{\theta\theta} = \mu \left(2 \left(\frac{1}{r} \frac{\partial W}{\partial \theta} + \frac{V}{r} \right) - \frac{2}{3} (\nabla \cdot \vec{v}) \right) \quad (12)$$

$$\tau_{zz} = \mu \left(2 \frac{\partial U}{\partial z} - \frac{2}{3} (\nabla \cdot \vec{v}) \right) \quad (13)$$

$$\tau_{r\theta} = \tau_{\theta r} = \mu \left(r \frac{\partial}{\partial r} \left(\frac{W}{r} \right) + \frac{1}{r} \frac{\partial V}{\partial \theta} \right) \quad (14)$$

$$\tau_{\theta z} = \tau_{z\theta} = \mu \left(\frac{\partial W}{\partial z} + \frac{1}{r} \frac{\partial U}{\partial \theta} \right) \quad (15)$$

$$\tau_{zr} = \tau_{rz} = \mu \left(\frac{\partial U}{\partial r} + \frac{\partial V}{\partial z} \right) \quad (16)$$

Where:

$$\nabla \cdot \vec{v} = \frac{\partial U}{\partial z} + \frac{\partial V}{\partial r} + \frac{V}{r} \quad (17)$$

- **Energy conservation**

The conservation of energy is the first law of thermodynamics, which, when applied to the moving fluid element

$$\frac{\partial T}{\partial t} + u_r \frac{\partial T}{\partial r} + \frac{u_\theta}{r} \frac{\partial T}{\partial \theta} + u_z \frac{\partial T}{\partial z} = \frac{\dot{q}_g}{cp} + \alpha \left[\frac{1}{r} \frac{\partial}{\partial r} \left(r \frac{\partial T}{\partial r} \right) + \frac{1}{r^2} \frac{\partial^2 T}{\partial \theta^2} + \frac{\partial^2 T}{\partial z^2} \right] + \frac{\Phi}{\rho cp} \quad (18)$$

Where the viscous rate of dissipation is

$$\Phi = 2\mu \left[\left(\frac{\partial u_r}{\partial r} \right)^2 + \left(\frac{1}{r} \frac{\partial u_\theta}{\partial \theta} + \frac{u_r}{r} \right)^2 + \left(\frac{\partial u_z}{\partial z} \right)^2 \right] + \mu \left[\left(\frac{1}{r} \frac{\partial u_r}{\partial \theta} + \frac{\partial u_\theta}{\partial r} - \frac{u_\theta}{r} \right)^2 + \left(\frac{\partial u_\theta}{\partial z} + \frac{1}{r} \frac{\partial u_z}{\partial \theta} \right)^2 + \left(\frac{\partial u_z}{\partial r} + \frac{\partial u_r}{\partial z} \right)^2 \right] \quad (19)$$

The turbulence model $k-\omega$ sst (Shear Stress Transfer) has been used because it is widely used when the state has a separation of flow and when using this model it takes into account the viscous sub-layer and distinguishes it from the rest of the layers for turbulent flow and this model is used in applications where simulation of thermal flow phenomena is required [13].

The general form of the equations is:

Kinematic eddy viscosity:-

$$\nu_T = \frac{\alpha_1 k}{\max(\alpha_1 \omega, S F_2)} \quad (20)$$

Where S is the average strain-rate

Turbulent kinetic energy

$$\frac{\partial k}{\partial t} + U_j \frac{\partial k}{\partial x_j} = P_k - \beta^* k \omega + \frac{\partial}{\partial x_j} \left[(\nu + \sigma_k \nu_T) \frac{\partial k}{\partial x_j} \right] \quad (21)$$

Specific dissipation rate:-

$$\frac{\partial \omega}{\partial t} + U_j \frac{\partial \omega}{\partial x_j} = \alpha S^2 - \beta \omega^2 + \frac{\partial}{\partial x_j} \left[(\nu + \sigma_\omega \nu_T) \frac{\partial \omega}{\partial x_j} \right] + 2(1 - F_1) \sigma_{\omega 2} \frac{1}{\omega} \frac{\partial k}{\partial x_i} \frac{\partial \omega}{\partial x_i} \quad (22)$$

The term $[2(1 - F_1) \sigma_{\omega 2} \frac{1}{\omega} \frac{\partial k}{\partial x_i} \frac{\partial \omega}{\partial x_i}]$ in Eq. (22) is a result of the transformation of the $k - \epsilon$ turbulence model to a $k - \omega$ formulation. The function F_1 is a blending function that ranged from one near the surface to zero far from the surface. Closure coefficients and auxiliary relations:-

$$P_k = \min \left(\tau_{ij} \frac{\partial U_i}{\partial x_j}, 10 \beta^* k \omega \right) \quad (23)$$

$$F_1 = \tanh \left\{ \left\{ \min \left[\max \left(\frac{\sqrt{k}}{\beta^* \omega y}, \frac{500 \nu}{y^2 \omega} \right), \frac{4 \sigma_{\omega 2} k}{C D_{k\omega} y^2} \right] \right\}^4 \right\} \quad (24)$$

$$F_2 = \tanh \left[\left[\max \left(\frac{2\sqrt{k}}{\beta^* \omega y}, \frac{500 \nu}{y^2 \omega} \right) \right]^2 \right] \quad (25)$$

$$C D_{k\omega} = \max \left(2 \rho \sigma_{\omega 2} \frac{1}{\omega} \frac{\partial k}{\partial x_i} \frac{\partial \omega}{\partial x_i}, 10^{-10} \right) \quad (26)$$

$$\alpha_1 = 5/9 \quad \alpha = 0.44 \quad , \quad \beta = \frac{3}{40} \quad , \quad \beta^* = \frac{9}{100} \quad , \quad \sigma_{\omega 2} = 0.856$$

Where: $\alpha_1, \alpha, \beta, \sigma_{\omega 2} =$ closure coefficients in the specific dissipation-rate equation and $\beta^* =$ closure coefficient in the turbulence-kinetic energy equation.

6. Results and Discussion

6.1. Numerical Validation

To ensure that the numerical solution that was carried out in this research correctly and the choice of simulating factors approximated to reality [14], a comparison must be made of the results obtained numerically with the theoretical results estimated from the Blasius solution for the friction factor and the number of Nusselt from the Dittus-Boelter equation (Eq. (2)), since the numerical values extracted for the friction factor It is from a Darcy-Weisbach equation (Eq. (4)). It is very clear that there is a compatibility between the numerical results from (ANSYS) and the results calculated from the experimental equations mentioned above and that the amount of deviation does not exceed 9 % as in Figures (7) and (8)

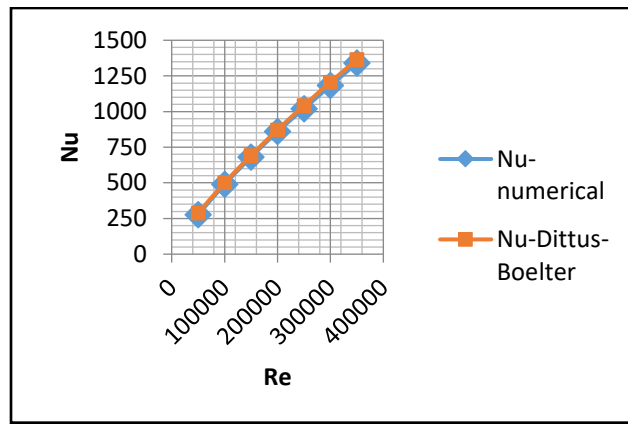


Figure 7. Validation of Nusselt number of smooth tube

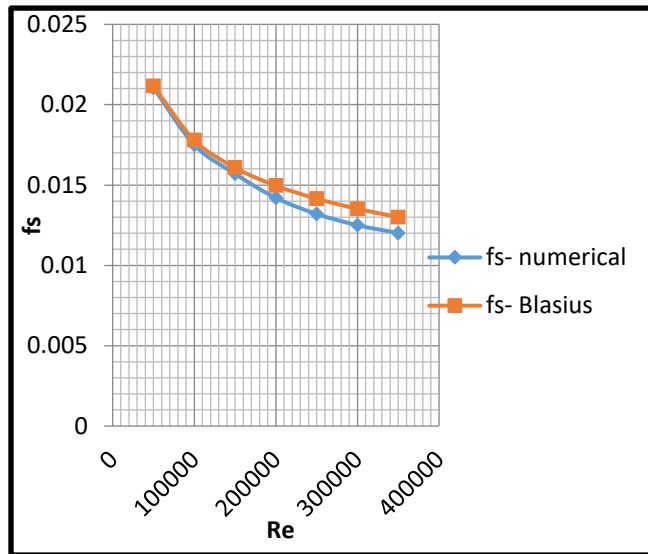


Figure 8. Validation of friction factor of smooth tube

6.2. The Structure of the Flow

The analysis of the flow structure in this research was done as in figure (9) to enhance the thermal performance factor of heat transfer, it is clear that there is an effect by the balls insert inside the water stream to improvement the heat transfer because of the velocity increase on both sides of the ball near the inner wall of the tube. Therefore; any increase in the velocity is offset by an increase in the convection heat transfer coefficient [15]. According to equation (1), the high speed leads to the blasting of the relative stagnation area near the wall.

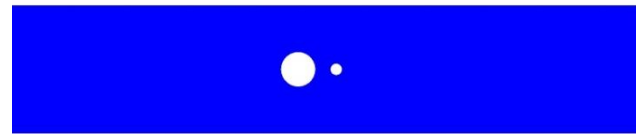


Figure 9. Flow structure for improvement thermal performance factor

6.3. Effect of Distance between the Balls (x)

From figure (10), it is clear to note the change of velocity on both sides of the large ball, the variable (x) which represents the distance between the large and small balls does not significantly affect the heat transfer because of the small size of the ball but rather affects the flow stream regulation, and this is evident through figure (11). Since the effect on increasing the amount of heat transferred is Reynolds number only. As the function of small ball is to reduce the amount of pressure drop, since, when an object blocks a path, it creates eddies behind the body due to the body’s non-flowing and these vortices cause a drop in pressure.

The case (x = 2mm) is where the entire small ball is inside the eddy space, which is the conical shape behind the large ball. As for the case (x = 3mm), the ball is outside eddies cone, but the effect of eddies increases negatively as the distance x increases as in the case (x = 5mm) because the small ball is relatively far away and does not eliminate or reduce eddies formed behind the large ball. And that the best of the previous cases is when (x = 2mm) as in Figure (12) where the pressure drop is minimal

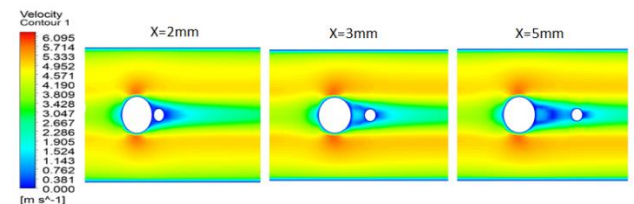


Figure 10. Velocity contour at different distances of (x)

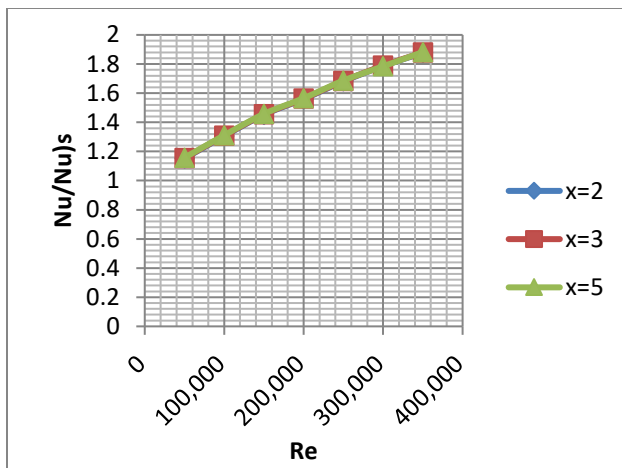


Figure 11. Nusselt ratio of tube with balls to smooth tube at (Dr=3)

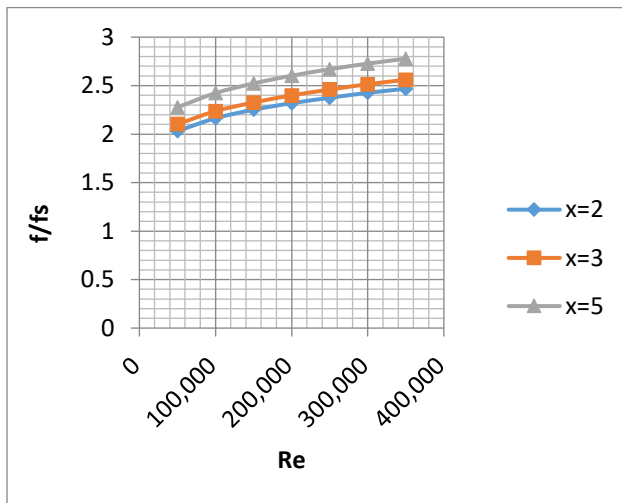


Figure 12. Friction factor ratio of tube with balls to smooth tube at (Dr=3)

6.4. Effect of Diameter Ratio (Dr)

If consideration is given to changing the size of the small ball with the same size as the large ball, then there will be a noticeable change in thermal performance, where there will be an increase in performance when increasing the size of the small ball when compared with cases for the same location until reach an increase in size which negatively affects performance. The pressure drop increases due to the eddies formed behind the large ball [16], the function of the small balls is the dispersal of these formed eddies, as in Figure (13). Where there is a difference of performance factor when the

diameter ratio is changed and the reason for this difference is that the small ball is located within the conical shaped of the eddies formed behind the large ball, if the ratio is large (that is, the small ball is small in size) then this does not result in any effect because the location of small ball is within the eddies cone.

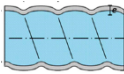
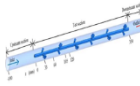
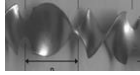
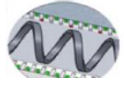
The change in the diameter ratio (Dr) (an increase in the size of the small ball), the greater its effect on the dispersal of eddies until the increase in size is not desirable because it leads to the formation of additional eddies that lead to additional pressure drop and this leads to a decrease in the thermal performance factor as in figure (14) and (15).

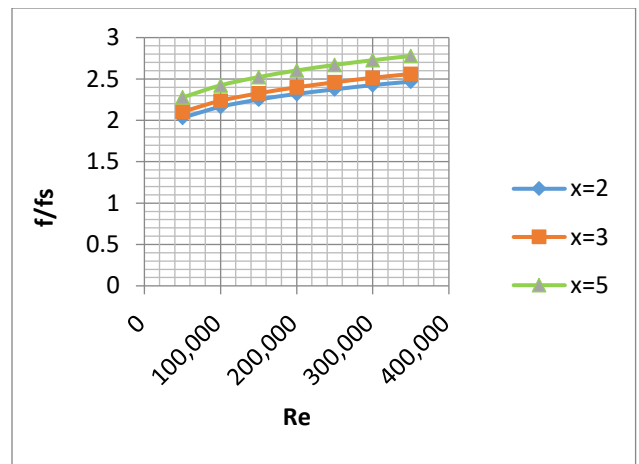
When the distance ($x = 2\text{mm}$), the performance factor has percentage increase by 16.8%, 17.6%, and 17% in the case of diameter ratio (Dr) is 3, 4, and 5, respectively, when consider the smooth tube has a unity performance factor. While at the distance ($x = 3\text{mm}$), the performance factor percentage increased by 15.7%, 17.4%, 17.8% when the diameter ratio (Dr) is equal to 3, 4, and 5, respectively. And when the distance ($x = 5\text{mm}$), the performance factor percentage increased by 12.8%, 14.1%, 14.7% when the diameter ratio (Dr) is equal to 3, 4, and 5, respectively. The values of thermal performance factor are shown in Table (1).

Table 1. thermal performance factor (η) at different distance (x) with variable diameter ratios

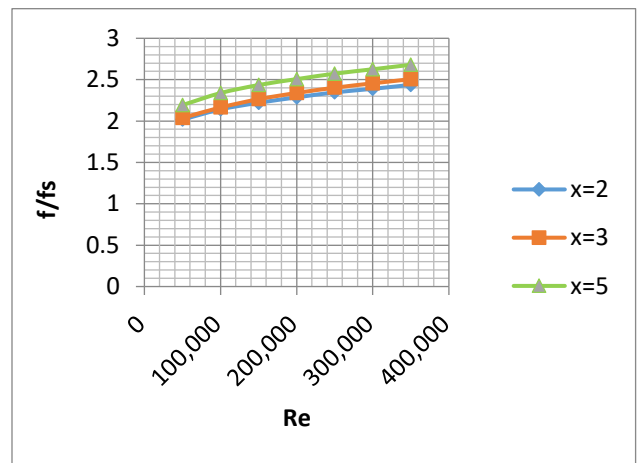
X[mm]	thermal performance factor (η)		
	Dr=3	Dr=4	Dr=5
2	1.168	1.176	1.17
3	1.157	1.174	1.178
5	1.128	1.141	1.147

Table 2. range of thermal performance factor (TPF) of previous studies

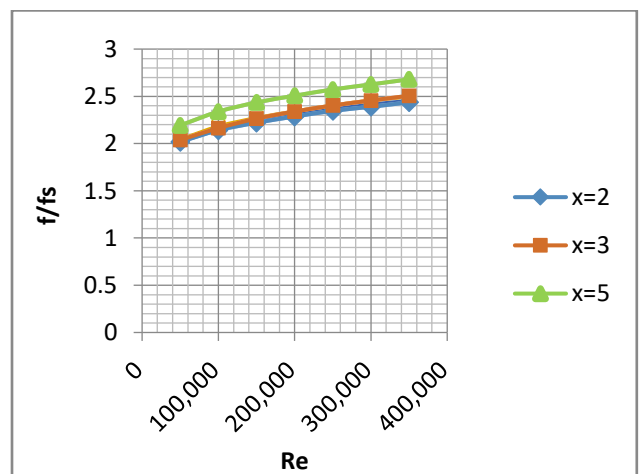
Researcher	Flow type	Range of Reynolds number	Thermal performance	Geometry
F. Andrade [7]	Transition flow	≥ 429 $Re \leq 6212$	~ 1.91 2.35	
Pengxiao Li [8]	Turbulent flow	$Re \geq 6000$ ≤ 16000	0.95 $1.04 \sim$	
Changzhong Man [9]	Turbulent flow	$3000 \leq Re$ ≤ 9000	1.02 \sim 1.42	
Shyy Woei Chang [10]	Turbulent flow	$\geq 10,000$ $Re \leq 40,000$	$1 \sim 0.7$ $3.$	



a) at diameter ratio (Dr=3)



b) at diameter ratio (Dr=4)



c) at diameter ratio (Dr=5)

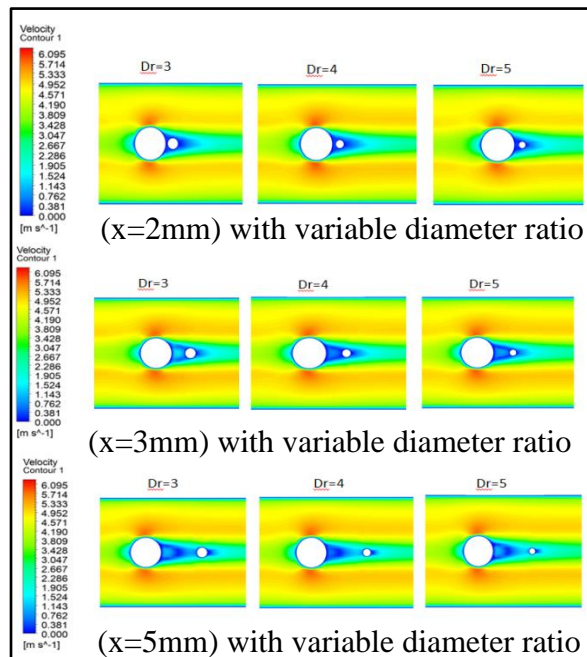
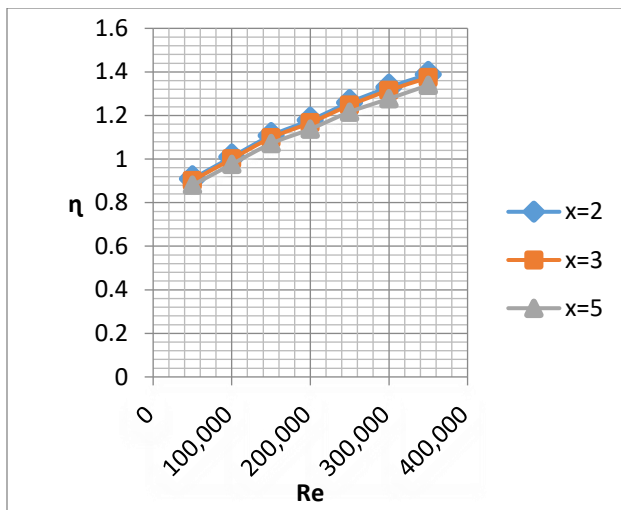
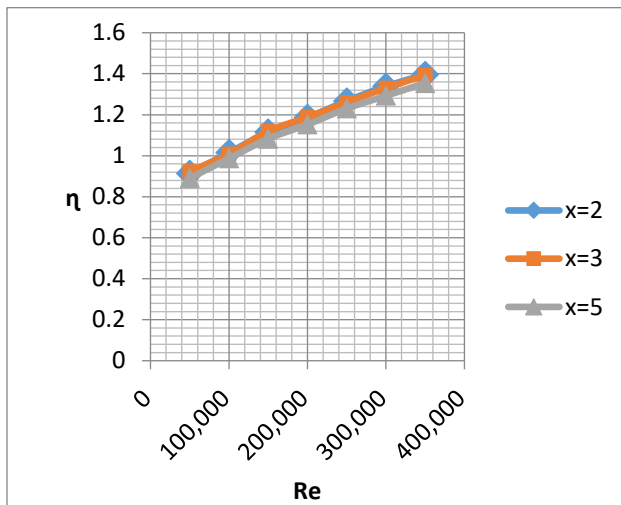


Figure 13. Velocity contour at different distances (x) with variable diameter ratios

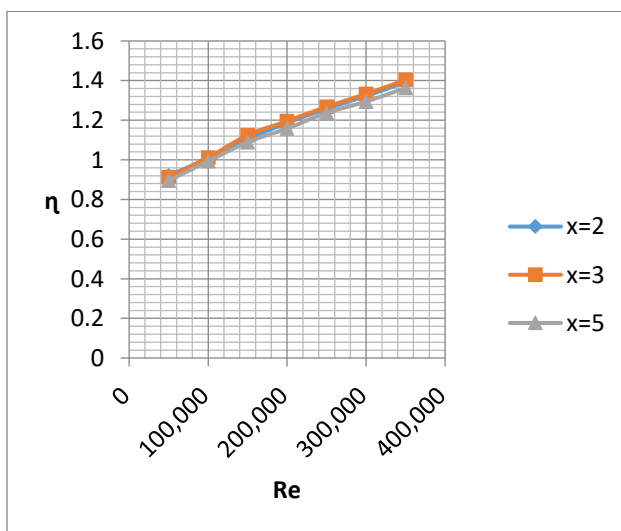
Figure 14. Friction factor ratio of tube with insert balls to smooth tube at different distances (x) with variable diameter ratios



a) diameter ratio (Dr=3)



b) diameter ratio (Dr=4)



(c) Diameter ratio (Dr=5)

Figure 15. Thermal performance factor

7. Conclusions

From the results reviewed, the following was concluded:

- 1- When adding geometric shapes inside the tube, it generally increases the thermal performance of the heat exchangers. Where the amount of the increase depends on the shape geometry, size, and number of balls.
- 2- In this research, two variables were studied numerically, the ratio of the diameter of two neighboring balls and the distance between them. It was found that in the two variables there is an effect on thermal performance factor (TPF).
- 3- When changing the distance between the small ball and the big ball, there is a slight change to the thermal performance factor, the higher the distance (x), the lower the value of the thermal performance factor.
- 4- The effect of the diameter ratio contributes significantly to increasing the value of the thermal performance factor by reducing the pressure drop in the flow as a result of the interception of the large ball of water flow, and this reduction occurs due to the dispersal of the eddies formed behind the large ball by the small ball.
- 5- Through the results obtained from the numerical solution, the best case was found among the cases studied in this research, which is at the highest value of the thermal performance factor (1.178). When compared to the smooth tube, the percentage of the increase in the thermal performance is (17.8%). Therefore, the results obtained numerically are reassuring when compared with previous studies.

Conflict of Interest

The authors confirm that the publication of this article causes no conflict of interest.

Nomenclature

D_r	Diameter ratio
X	Distance between large and small balls [mm]
D_b	Diameter of large ball [mm]
D_{sb}	Diameter of small ball [mm]
Re	Reynolds number
TPF	Thermal Performance Factor (η)
D_t	Tube diameter [mm]
k	specific turbulence kinetic energy
L	Distance between two large balls [mm]
Nu	Nusselt number
Nu_s	Nusselt number of smooth tube
h	Convection heat transfer coefficient [W/m ² .K]
λ	Thermal conductivity of fluid [W/m.K]
Pr	Prandtl number
P_k	production of turbulence kinetic energy
τ_{ij}	specific Reynolds-stress tensor
ρ	Density [kg/m ³]
u	Average velocity of the fluid [m/s]
f	Friction factor
f_s	Friction factor of smooth tube
Δp	Pressure drop
ω	specific dissipation rate
η	Thermal performance factor (TPF)

8. References

- 1- R. L. Webb and E. R. G. Eckert (1972) "Application of rough surfaces to heat exchanger design," *International Journal of Heat and Mass Transfer* vol. 15, no. 9, pp. 1647–1658.
- 2- Rajendra Karwa, Chandresh Sharma, and Nitin Karwa (2013) "Performance Evaluation Criterion at Equal Pumping Power for Enhanced Performance Heat Transfer Surfaces" Hindawi Publishing Corporation Journal of Solar Energy Volume 2013
- 3- Kyung Min Kim, Beom Seok Kim, Dong Hyun Lee, Hokyung Moon, Hyung Hee Cho (2010) "Optimal design of transverse ribs in tubes for thermal performance enhancement" *Energy* 35, 2400–2406.
- 4- Xin-Yi Tanga, Dong-Sheng Zhu (2013), "Flow structure and heat transfer in a narrow rectangular channel with different discrete rib arrays" *Chem. Eng. Process.* 69.14–1
- 5- Jasin' ski. Piotr (2012) "Numerical study of friction factor and heat transfer characteristics for single-phase turbulent flow in tubes with helical microfins" *Arch. Mech. Eng.* LIX (4) 469–485.
- 6- F. Andrade, A.S. Moita, A. Nikulin, A.L.N. Moreira, H. Santosb (2019) "Experimental investigation on heat transfer and pressure drop of internal flow in corrugated tubes" *International Journal of Heat and Mass Transfer*
- 7- Pengxiao Li, Peng Liu, Zhichun Liu, Wei Liu (2017) "Experimental and numerical study on the heat transfer and flow performance for the circular tube fitted with drainage inserts" *International Journal of Heat and Mass Transfer* 107, 686–696.
- 8- C. Man et al. (2016) "Experimental study on effect of heat transfer enhancement for

- single-phase forced convective flow with twisted tape inserts*” Int. J. Heat Mass Transfer.10.026
- 9- Shyy Woei Chang , Jing Yan Gao, Hung Lin Shih (2015) “*Thermal performances of turbulent tubular flows enhanced by ribbed and grooved wire coils*” International Journal of Heat and Mass Transfer 90, 1109–1124
- 10- Piotr Bogusław Jasin´ ski (2017) “*Numerical study of thermo-hydraulic characteristics in a circular tube with ball turbulators. Part 3: Thermal performance analysis*” International Journal of Heat and Mass Transfer 107, 1138–1147
- 11- Jasin´ ski. Piotr (2012) “*Numerical study of friction factor and heat transfer characteristics for single-phase turbulent flow in tubes with helical microfins*” Arch. Mech. Eng. LIX (4) 469–485.
- 12- Versteeg HK and Malalasekera V, 2007. *An Introduction to Computational Fluid Dynamics: The Finite Volume Method*, Second Edition, Pearson Education Limited 1995, 2007
- 13- S.R. Shabaniyan, M. Rahimi, M. Shahhosseini, A.A. Alsairafi (2011) “*CFD and experimental studies on heat transfer enhancement in an air cooler equipped with different tube inserts*” Int. Commun. Heat Mass Transfer 38, 383–390.
- 14- Jasin´ ski Piotr (2014) “*Numerical study of the thermal–hydraulic characteristics in a circular tube with ball turbulators. Part 2: Heat transfer and efficiency indexes*” Int. J. Heat Mass Transfer 74 473–483.
- 15- A. Hadidi, M. Hadidi, A. Nazari (2013) “*A new design approach for shell-and-tube heat exchangers using imperialist competitive algorithm (ICA) from economic. point of view, Energy Convers*” Manag. 67, 66e74.
- 16- Shailesh Jindal, Lyle N. Long (2004) “*large eddy simulation around a sphere using unstructured grids*” 34th AIAA Fluid Dynamics Conference and Exhibit, Portland, Oregon.